Annals of the University of Craiova, Mathematics and Computer Science Series
Volume 49(2), 2022, Pages 291–308, DOI: 10.52846/ami.v49i2.1560
ISSN: 1223-6934

A Modified Susceptible-Infected-Recovered Epidemiological Model

Ion Bica, Zhichun Zhai, and Rui Hu

Abstract.
Objectives
This paper proposes an infectious disease model incorporating two new model compartments, hospitalization, and intensive care unit.
Methods
The model dynamics are analyzed using the local and global stability theory of nonlinear systems of ordinary differential equations. For the numerical simulations, we used the Rosenbrock method for stiff initial value problems. We obtained numerical simulations using MAPLE software. The returned MAPLE procedure was called only for points inside the range on which the method evaluated the numerical solution of the system with specified initial conditions.
Results
- We proposed a new model to describe the dynamics of microparasitic infections.
- Numerical simulations revealed that the proposed model fitted with the expected behaviour of microparasitic infections with "acute epidemicity."
- The numerical simulations showed consistency in the behaviour of the system.

Conclusions
- The model proposed has "robust" dynamics, supported by the global stability of its endemic state and the consistency of the numerical simulations regarding the model's time evolution behaviour.
- The introduction of the hospitalization and intensive care unit compartments in the proposed model revealed that it is essential to consider such policies in the case of "acute epidemicity" of microparasitic infections.

2010 Mathematics Subject Classification. Primary 34D23, 37M05, 37N25; Secondary 92C50.
Key words and phrases. micro-parasitic infection, acute epidemicity, SIR model, endemic equilibrium, local stability, global stability.

1. Introduction

The SIR model is a classical model for studying the dynamics of infectious diseases introduced by Kermack and McKendrick in 1927 [13] following prior works conducted by Ross and Hudson [21] [22] [23]. Ronald Ross [21] gives a relevant, intuitive classification of infectious diseases, classifying the pandemic-type of diseases, based on their "acute epidemicity," separately from any other types of infectious diseases. In that perspective, COVID 19 fits the profile of being a pandemic-type of infectious disease. We designed a model addressing the "acute epidemicity" of an infectious disease primarily, which can be applied to any disease within this class, including COVID 19. In designing our model, we followed the expected findings of Ross [22] looking for

Received October 13, 2021. Accepted October 25, 2022 .
This research is supported by the Natural Sciences and Engineering Research Council of Canada.

solutions whose graphs "are bell-shaped and nearly symmetrical, and tend to decline more slowly than they rose." Based on Ross' intuitive classification, we show that the model that we propose behaves in the way described by Ross, but the disease may not disappear. We will have two scenarios for the equilibrium states of the model. One scenario when we have only the disease-free equilibrium state and the second scenario when besides the disease-free equilibrium state, we have an endemic equilibrium state, suggesting that the disease did not "disappear entirely after the acute epidemicity." Therefore, we extend the class of infectious diseases with "acute epidemicity" described by Ross to the class of diseases as presented by Hethcote [10] "Classification of infectious diseases by agent and mode of transmission," where the SIR model is applicable. The mathematical understanding of the dynamics of infectious diseases is a persistent endeavour by many researchers in the field; [1] [10] [11] [15] are a few examples of works by experts in the field of modeling infectious diseases.

The following system of ordinary differential equations describes the classical epidemic model for microparasitic infections (i.e., caused by bacteria or viruses) [11]

$$\begin{aligned} \frac{dS}{dt} &= -\beta SI, \\ \frac{dI}{dt} &= \beta SI - \gamma_I I, \\ \frac{dR}{dt} &= \gamma_I I. \end{aligned} \tag{1.1}$$

where $S(t)$, $I(t)$, and $R(t)$ represent the number of susceptible, infected, and recovered individuals at time t, β is the transmission rate of the disease, and γ_I is the recovery rate of infected individuals. The model (1.1) is called a compartmentalized model where the three compartments, S, I, and R are assumed to be homogeneously mixed, i.e., there are no separations amongst the three compartments at any time. The assumptions on which the model (1.1) is based are the followings:

- The system is closed. The total size of the population considered for the model is constant, i.e., $N = S + I + R = constant$, as $\frac{dS}{dt} + \frac{dI}{dt} + \frac{dR}{dt} = 0$.
- The first equation indicates that the rate at which the susceptible individuals become infected is proportional to the number of susceptible individuals that come in contact with the infected individuals; this gives the rationale of the term βSI.
- The third equation indicates that the rate at which the recovered individuals become immune to the disease (i.e., unable to transmit the disease) is proportional to the number of infected individuals.

In the model that we propose, we modify the SIR model (1.1) by first introducing the following new variables (new compartments):

- $H(t)$ representing the number of hospitalized individuals who do not require to be in the Intensive Care Unit (ICU).
- $U(t)$ representing the number of hospitalized individuals in ICU.
- $D(t)$ representing the deceased individuals (cumulative) due to the infection.

The compartment D is a standard variable in epidemiological modeling. It has high relevance, especially for the pandemic-type of infectious diseases where the mortality factor is an essential component to consider. The SIR epidemic model including the compartment D is called $SIRD$ model, and [2] [3] [16] [19] are a few examples that address pandemic-type of infectious diseases; COVID 19.

For pandemic-type of infectious diseases, the rapidly increasing frequency of hospitalization and ICU are significant variables of the proposed model, as the COVID 19 reality revealed.

We propose the following autonomous system of differential equations, a Susceptible - Infected - Hospitalized - (Intensive Care) Unit - Recovered - Deceased model ($SIHURD$)

$$\begin{aligned}
\frac{dS}{dt} =& \tau N - \frac{\beta}{N} SI - \tau S, \\
\frac{dI}{dt} =& \frac{\beta}{N} SI - (\gamma_I + \nu + \eta + \mu_I + \tau) I, \\
\frac{dH}{dt} =& \nu I - (\tau + \gamma_H + \mu_H) H, \\
\frac{dU}{dt} =& \eta I - (\tau + \gamma_U + \mu_U) U, \\
\frac{dR}{dt} =& \alpha_I \gamma_I I + \alpha_H \gamma_H H + \alpha_U \gamma_U U - \tau R, \\
\frac{dD}{dt} =& \mu_I I + \mu_H H + \mu_U U - dD.
\end{aligned} \tag{1.2}$$

- N : initial alive human population size.
- β : transmission rate of disease from an infected individual to a susceptible individual; same meaning as for the SIR model (1.1).
- τ : natural mortality rate of human individuals assumed constant for each country.
- γ_I : global average recovery rate over all infected individuals.
- γ_H : global average recovery rate over all hospitalized individuals who do not require being in ICU.
- γ_U : global average recovery rate over all individuals who require being in ICU.
- α_I : dimensionless multiple of γ_I indicating the expected recovery rate of each infected individuals specific to the unit of time used. $\alpha_I \in (0, 1]$, with $\alpha_I = 1$ when the recovery of an infected individual from the compartment I is completed.
- α_H : dimensionless multiple of γ_H indicating the expected recovery rate of each infected individuals specific to the unit of time used. $\alpha_H \in (0, 1]$, with $\alpha_H = 1$ when the recovery of an infected individual from the compartment H is completed.
- α_U : dimensionless multiple of γ_U indicating the expected recovery rate of each infected individuals specific to the unit of time used. $\alpha_U \in (0, 1]$, with $\alpha_U = 1$ when the recovery of an infected individual from the compartment U is completed.
- ν : rate of infected individuals who need to be hospitalized but do not require being in ICU.
- η : rate of infected individuals who require being in ICU.
- μ_I : microparasitic-induced averaged fatality rate of infected individuals.
- μ_H : microparasitic-induced averaged fatality rate of hospitalized individuals who were not in ICU.
- μ_U : microparasitic-induced averaged fatality rate of individuals deceased in ICU.

- $1/d$: mean caring duration of deceased human individuals. Thus, d denotes the burial rate of deceased human individuals (i.e., natural death rate). Here, we assume that $d \geq \tau$.

The $SIHURD$ model (1.2) takes in account the following assumptions:

- It has vital dynamics [11]: we consider that the death balances the birth at a constant rate τ, so we take into account the inflow of newborns into the susceptible compartment at rate τN and deaths in the compartments S, I, H, U, and R at rates τS, τI, τH, τU, and τR respectively. As well, according to [12] infants can become infected with the virus that causes COVID-19.
- The system is not closed because we take in account the burial rate, d. Thus, the rate at which the total population varies (including death as well) is given by

$$\frac{d}{dt}\left(S+I+H+U+R+D\right) =$$

$$\tau\left[N-\left(S+I+H+U+R\right)\right]-\left(1-\alpha_I\right)I-\left(1-\alpha_H\right)H-\left(1-\alpha_U\right)U-dD. \quad (1.3)$$

  Without the burial rate d, and when all infected population is recovered, i.e., $\alpha_I = \alpha_H = \alpha_U = 1$, considering the system (1.2) with $N = S(t) + I(t) + H(t) + U(t) + R(t)$, then the system would be closed. Indeed, we would have

$$\frac{d}{dt}\left(S+I+H+U+R+D\right)=0 \;\Rightarrow\; S+I+H+U+R+D = constant. \quad (1.4)$$

  which proves the consistency of our modeling with respect to the SIR classic endemic model [11]. Our assumption is based on the fact that mortality happens regardless of epidemic microparasitic infections.

In the subsequent sections, we will discuss the theoretical aspect of the model (1.2) and numerical simulations exemplifying the behaviour of the model. Lastly, we will summarize our results showing how they suit a pandemic-type scenario for microparasitic infections.

2. Equilibrium states and nullclines

The dynamical system (1.2) has an endemic equilibrium point

$$\begin{aligned}
\hat{S} &= \frac{N}{R_0},\\
\hat{I} &= \frac{\tau N(R_0-1)}{\beta},\\
\hat{H} &= \frac{\nu\tau N(R_0-1)}{\beta\sigma_H},\\
\hat{U} &= \frac{\eta\tau N(R_0-1)}{\beta\sigma_U},\\
\hat{R} &= \frac{N(R_0-1)(\eta\alpha_U\gamma_U\sigma_H+\nu\alpha_H\gamma_H\sigma_U+\alpha_I\gamma_I\sigma_H\sigma_U)}{\beta\sigma_H\sigma_U},\\
\hat{D} &= \frac{\tau N(R_0-1)(\eta\mu_U\sigma_H+\nu\mu_H\sigma_U+\mu_I\sigma_H\sigma_U)}{\beta d\sigma_H\sigma_U},
\end{aligned} \quad (2.1)$$

where

$$R_0 = \frac{\beta}{\gamma_I + \nu + \eta + \mu_I + \tau},\ \sigma_H = \gamma_H + \mu_H + \tau,\ \sigma_U = \gamma_U + \mu_U + \tau, \tag{2.2}$$

if

$$R_0 = \frac{\beta}{\gamma_I + \nu + \eta + \mu_I + \tau} > 1. \tag{2.3}$$

If $R_0 \leq 1$ the dynamical system (1.2) has only the disease-free equilibrium point

$$S = N,\ I = 0,\ H = 0,\ U = 0,\ R = 0,\ D = 0. \tag{2.4}$$

The number R_0 in (2.3) is called reproduction number and explanations regarding it can be found in [28] & [6].

In this article, we are interested in discussing the dynamical system (1.2) when it has an endemic equilibrium point, i.e., $R_0 > 1$.

The dynamics of the two compartments S and I in the $SIHURD$ model (1.2) is independent of the dynamics of the compartments H, U, R, and D, i.e., they behave like a self-contained system within the $SIHURD$ system. Thus, their dynamics will be unchanged within the dynamics of the whole system (1.2). But the compartment I will affect the dynamics of the other components of the system (1.2), H, U, R, and D, respectively.

The directional vector field for the compartments S and I in (1.2), when $S \neq 0$, is

$$\vec{F} = F_S\vec{i} + F_I\vec{j}, \tag{2.5}$$

where

$$\begin{aligned} F_S =& \beta S\left[\frac{\tau}{\beta}\left(\frac{N}{S} - 1\right) - \frac{I}{N}\right], \\ F_I =& \beta I\left(\frac{S}{N} - \frac{1}{R_0}\right). \end{aligned} \tag{2.6}$$

From (2.6) we get the S-nullcline and the I-nullcline, respectively

$$\begin{aligned} I =& \frac{\tau N}{\beta}\left(\frac{N}{S} - 1\right), \\ S =& \frac{N}{R_0}. \end{aligned} \tag{2.7}$$

Based on the nullclines (2.7), the $(S,\ I)$ components of the endemic equilibrium point (2.1) represent always a stable equilibrium point in the $S - I$ solution plane. Indeed we have

$$\begin{aligned} &F_S < 0 \text{ for } I > \frac{\tau N}{\beta}\left(\frac{N}{S} - 1\right), \\ &F_S > 0 \text{ for } I < \frac{\tau N}{\beta}\left(\frac{N}{S} - 1\right), \\ &F_I < 0 \text{ for } S < \frac{N}{R_0}, \\ &F_I > 0 \text{ for } S > \frac{N}{R_0}. \end{aligned} \tag{2.8}$$

Figure 1 is a generic picture showing the nullclines (2.7) that reveal the dynamics of the two compartments S and I in the $SIHURD$ model (1.2). Based on (2.8), the trajectories of S and I will always have the tendency to merge towards the equilibrium point

$$\begin{aligned} \hat{S} &= \frac{N}{R_0}, \\ \hat{I} &= \frac{\tau N(R_0 - 1)}{\beta}, \end{aligned} \tag{2.9}$$

in the $S-I$ solution plane. Based on the explanations that we gave above regarding the dynamics of the compartments S and I, we notice, as expected, that the equilibrium point (2.9) is the same as $\hat{S}$ and $\hat{I}$ in (2.1).

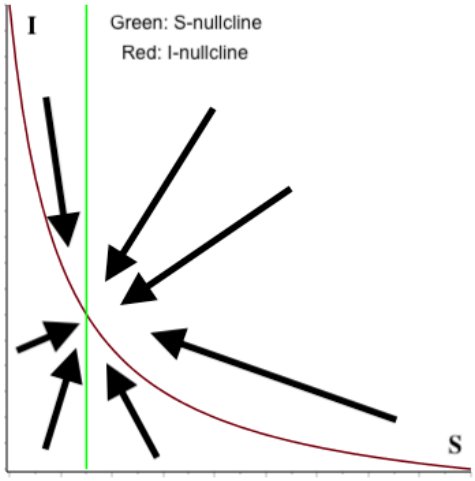

FIGURE 1. The nullclines (2.7), the equilibrium point (2.9), and the behavior the the vector field (2.5) as revealed in (2.8).

In the next section we discuss about the local stability of the equilibrium point (2.9). We will show that it is asymptotically stable, followed by a proof of its global asymptotic stable behaviour.

3. Local and global stability of the equilibrium point (2.9)

Linearizing the system

$$\begin{aligned} \frac{dS}{dt} &= \tau N - \frac{\beta}{N} SI - \tau S, \\ \frac{dI}{dt} &= \frac{\beta}{N} SI - \frac{\beta}{R_0} I, \end{aligned} \tag{3.1}$$

about its equilibrium point (2.9), we obtain the following Jacobian matrix representing the coefficient matrix of the linearized system of (3.1) about its equilibrium point (2.9)

$$J_{SI} = \begin{bmatrix} -\tau R_0 & -\frac{\beta}{R_0} \\ \tau(R_0 - 1) & 0 \end{bmatrix}, \tag{3.2}$$

with the following eigenvalues

$$\lambda_{1,2} = \frac{1}{2}\frac{-\tau R_0^2 \pm \sqrt{\tau^2 R_0^4 - 4\beta\tau R_0^2 + 4\beta\tau R_0}}{R_0}. \tag{3.3}$$

Because we work under the case $R_0 > 1$, then

$$\tau R_0^2 > \sqrt{\tau^2 R_0^4 - 4N\beta\tau R_0^2 + 4N\beta\tau R_0}. \tag{3.4}$$

Thus, $Re(\lambda_{1,2}) < 0$, which shows that the equilibrium point (2.9) is an asymptotically stable hyperbolic point. The equilibrium point (2.9) is

- Asymptotically stable node if $Im(\lambda_{1,2}) = 0$.
- Asymptotically stable focus if $Im(\lambda_{1,2}) \neq 0$.

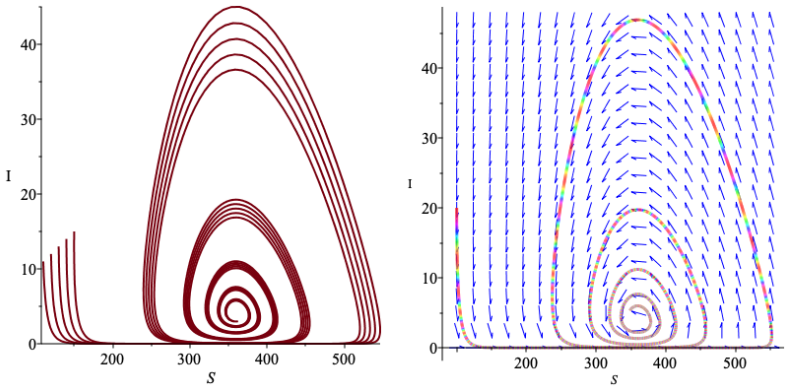

(A) Trajectories of the system (3.1) with initial conditions $S(0) = 10(10+i)$, $I(0) = 10+i$, $i = 1..5$.

(B) Phase portrait and trajectory of the system (3.1) with initial conditions $S(0) = 100$, $I(0) = 20$.

FIGURE 2. Phase portrait and trajectories for the system (3.1) on the time range $t = 0..2500$ for $N = 1000$, $\tau = 0.001$, $\beta = 0.4417$, $\nu = 0.013$, $\eta = 0.001$, $\gamma_I = 0.1384$, and $\mu_I = 0.00542$.

Figure 2 shows the dynamics of the system (3.1) in a scenario of infection spread at a rate $\beta = 0.4417$/unit time within a community of individuals $N = 1000$ with a natural mortality rate (measured per 1000 population) $\tau = 0.001$ (i.e., the rate of natural death is 0.1%) throughout 2500 units of time. We considered the rate of hospitalization of individuals not requiring to be in ICU, $\nu = 0.013$/unit time, and the rate of infected individuals needing to be in ICU, $\eta = 0.001$/unit time. Lastly, we considered the recovery rate of infected individuals, $\gamma_I = 0.1384$/unit time, and the fatality rate due to infection, $\mu_I = 0.00542$/unit time. Thus, the trajectories of the system will approach the equilibrium state given by the equilibrium point (2.9), which, for this scenario, is an asymptotically stable focus.

Let us notice from Figure 2 that if we started with nonnegative initial conditions, $S(0) = S_0 \geq 0$ & $I(0) = I_0 \geq 0$, then $S(t) \geq 0$ & $I(t) \geq 0$ for all $t \geq 0$. Indeed, let us show that every time when the initial conditions for the system (3.1) are nonnegative, then the trajectories of the system will be residing in $\mathbb{R}^2_+$.

Theorem 3.1. *If $S(0) = S_0 \geq 0$ & $I(0) = I_0 \geq 0$, then the trajectories of the system (3.1) will reside in $\mathbb{R}^2_+$, i.e., $S(t) \geq 0$ & $I(t) \geq 0$ for all $t \geq 0$.*

Proof. The first equation of the system (3.1) can be viewed as a first order ordinary differential equation in standard form as follows

$$\frac{dS}{dt} + P(t)S + Q(t) = 0, \;\; P(t) = \frac{\beta}{N} I(t) + \tau, \;\; Q(t) = -\tau N. \tag{3.5}$$

The equation (3.5), under the initial condition $S(0) = S_0$, has the unique solution

$$S(t) = e^{-\int_0^t \left(\frac{\beta}{N} I(w) + \tau\right) dw} \int_0^t \tau N e^{-\int_0^t \left(\frac{\beta}{N} I(w) + \tau\right) dw} \, dv + S_0 e^{-\int_0^t \left(\frac{\beta}{N} I(w) + \tau\right) dw}. \tag{3.6}$$

If $S_0 \geq 0$, from (3.6), it follows immediately that $S(t) \geq 0$ for all $t \geq 0$.

The second equation of the system (3.1) can be viewed as a separable ordinary differential equation in the variable I as follows

$$\frac{dI}{I} = \beta \left(\frac{S}{N} - \frac{1}{R_0} \right). \tag{3.7}$$

The equation (3.7), under the initial condition $I(0) = I_0$, has the unique solution

$$I(t) = I_0 e^{\int_0^t \beta \left(\frac{S(w)}{N} - \frac{1}{R_0} \right) dw}. \tag{3.8}$$

If $I_0 \geq 0$, from (3.8), it follows immediately that $I(t) \geq 0$ for all $t \geq 0$. □

Regarding the global stability of the equilibrium point (2.9), we will prove it through the following theorem.

Theorem 3.2. *The endemic equilibrium point (2.9) is globally asymptotically stable.*

Proof. Following the ideas from [14] & [26], let us define the following function

$$V(S, I) = S - \hat{S} - \hat{S} \ln \left(\frac{S}{\hat{S}} \right) + I - \hat{I} - \hat{I} \ln \left(\frac{I}{\hat{I}} \right), \tag{3.9}$$

on some neighbourhood U of $\left(\hat{S}, \hat{I}\right)$. Because the set $U \setminus \left\{ \left(\hat{S}, \hat{I}\right) \right\}$ cannot be empty, it is important to note that we work under the assumption that the endemic equilibrium point $\left(\hat{S}, \hat{I}\right)$ satisfies $\hat{S} > 1$ and $\hat{I} > 1$.

The function V satisfies the following properties

- V is C^1 on U,
- $V\left(\hat{S}, \hat{I}\right) = 0$,
- $V(S, I) > 0$ for all $(S, I) \in U \setminus \left\{ \left(\hat{S}, \hat{I}\right) \right\}$. We have

$$\nabla V = \left[1 - \frac{N}{R_0 S}, \; 1 - \frac{\tau N (R_0 - 1)}{\beta I} \right]^T, \tag{3.10}$$

which show that the only critical point of V is the endemic equilibrium point $\left(\hat{S}, \hat{I}\right)$, and $V\left(\hat{S}, \hat{I}\right) = 0$ is the absolute minimum of V in any neighbourhood U of $\left(\hat{S}, \hat{I}\right)$. Therefore $V(S, I) > 0$ for all $(S, I) \in U \setminus \left\{ \left(\hat{S}, \hat{I}\right) \right\}$.

As well, let us prove that

$$\dot{V} = \nabla V \cdot \left[\dot{S}, \dot{I}\right]^T < 0,\ \forall (S, I) \in U \setminus \left\{\left(\hat{S}, \hat{I}\right)\right\}. \tag{3.11}$$

Indeed, using (3.10) and the equations in (3.1) we obtain

$$\nabla V \cdot \left[\dot{S}, \dot{I}\right]^T = -\frac{\tau(N - R_0 S)^2}{R_0 S} < 0,\ \forall (S, I) \in U \setminus \left\{\left(\hat{S}, \hat{I}\right)\right\},$$

which shows that (3.11) is true.

Hence, the function V defined in (3.9) is a strict Lyapunov function, therefore the endemic equilibrium point (2.9) is globally asymptotically stable. □

4. Local and global stability of the equilibrium point (2.1)

Linearizing the system (1.2) about its equilibrium point (2.1), we obtain the following Jacobian matrix representing the coefficient matrix of the linearized system of (1.2) about its equilibrium point (2.1).

$$J = \begin{bmatrix} -\tau R_0 & -\frac{\beta}{R_0} & 0 & 0 & 0 & 0 \\ \tau(R_0 - 1) & 0 & 0 & 0 & 0 & 0 \\ 0 & \nu & -\sigma_H & 0 & 0 & 0 \\ 0 & \eta & 0 & -\sigma_U & 0 & 0 \\ 0 & \alpha_I\gamma_I & \alpha_H\gamma_H & \alpha_U\gamma_U & -\tau & 0 \\ 0 & \mu_I & \mu_H & \mu_U & 0 & -d \end{bmatrix}, \tag{4.1}$$

with the following eigenvalues

$$\lambda_{1,2} = \frac{1}{2}\frac{-\tau R_0^2 \pm \sqrt{\tau^2 R_0^4 - 4\beta\tau R_0^2 + 4\beta\tau R_0}}{R_0},$$
$$\lambda_3 = -\sigma_H,\ \lambda_4 = -\sigma_U,\ \lambda_5 = -\tau,\ \lambda_6 = -d. \tag{4.2}$$

Because we work under the case $R_0 > 1$ (when we have an endemic equilibrium state), then

$$\tau R_0^2 > \sqrt{\tau^2 R_0^4 - 4\beta\tau R_0^2 + 4\beta\tau R_0},$$

and therefore $Re(\lambda_{1,2}) < 0$. As well, we have $\lambda_i < 0$, $i = 3..6$. Thus, the equilibrium point (2.1) is an asymptotically stable hyperbolic point.

As an important note, based on the explanations that we gave in Section 2 regarding the dynamics of the compartments S and I, we notice, as expected, that the eigenvalues $\lambda_{1,2}$ in (4.2) are the same as the eigenvalues $\lambda_{1,2}$ in (3.3).

Theorem 4.1. *If $S(0) = S_0 \geq 0$, $I(0) = I_0 \geq 0$, $H(0) = H_0 \geq 0$, $U(0) = U_0 \geq 0$, $R(0) = S_0 \geq 0$, & $D(0) = D_0 \geq 0$, then the trajectories of the system (1.2) will reside in $\mathbb{R}^6_+$.*

Proof. The proof of $S(t) \geq 0$ & $I(t) \geq 0$ for all $t \geq 0$ is identical with the proof given in the Theorem 3.1. Let us prove that $H(t) \geq 0$ & $U(t) \geq 0$ for all $t \geq 0$.

The third and fourth equations of the system (1.2) can be viewed as first order ordinary differential equations in standard form, as follows

$$\frac{dH}{dt} + P(t)H + Q(t) = 0,\ P(t) = \sigma_H,\ Q(t) = -\nu I(t),\ \sigma_H = \tau + \gamma_H + \mu_H, \tag{4.3}$$

$$\frac{dU}{dt} + P(t)U + Q(t) = 0,\ P(t) = \sigma_U,\ Q(t) = -\eta I(t),\ \sigma_U = \tau + \gamma_U + \mu_U. \tag{4.4}$$

The equations (4.3) and (4.4), under the initial conditions $H(0) = H_0$ and $U(0) = U_0$ respectively, have the following unique solutions

$$H(t) = e^{-\sigma_H t}\int_0^t e^{\sigma_H w}\nu I(w)\,dw + e^{-\sigma_H t}H_0, \tag{4.5}$$

$$U(t) = e^{-\sigma_U t}\int_0^t e^{\sigma_U w}\eta I(w)\,dw + e^{-\sigma_U t}U_0. \tag{4.6}$$

If $H_0 \geq 0$ and $U_0 \geq 0$, and because $I(t) \geq 0$ for all $t \geq 0$, from (4.5) and (4.6), it follows immediately that $H(t) \geq 0$ & $U(t) \geq 0$ for all $t \geq 0$.

The fifth and sixth equations of the system (1.2) can be viewed as first order ordinary differential equations in standard form, as follows

$$\frac{dR}{dt} + P(t)R + Q(t) = 0,\ P(t) = \tau,\ Q(t) = -\left(\alpha_I\gamma_I I(t) + \alpha_H\gamma_H H(t) + \alpha_U\gamma_U U(t)\right), \tag{4.7}$$

$$\frac{dD}{dt} + P(t)D + Q(t) = 0,\ P(t) = d,\ Q(t) = -\left(\mu_I I(t) + \mu_H H(t) + \mu_U U(t)\right). \tag{4.8}$$

The equations (4.7) and (4.8), under the initial conditions $R(0) = R_0$ and $D(0) = D_0$ respectively, have the following unique solutions

$$R(t) = e^{-\tau t}\int_0^t e^{\tau w}\left(\alpha_I\gamma_I I(w) + \alpha_H\gamma_H H(w) + \alpha_U\gamma_U U(w)\right)\,dw + e^{-\tau t}R_0, \tag{4.9}$$

$$D(t) = e^{-dt}\int_0^t e^{dw}\left(\mu_I I(w) + \mu_H H(w) + \mu_U U(w)\right)\,dw + e^{-dt}D_0. \tag{4.10}$$

If $R_0 \geq 0$ and $D_0 \geq 0$, and because $I(t) \geq 0$, $H(t) \geq 0$, and $U(t) \geq 0$ for all $t \geq 0$, from (4.9) and (4.10), it follows immediately that $R(t) \geq 0$ & $D(t) \geq 0$ for all $t \geq 0$.

Hence, under nonnegative initial conditions, the trajectories of the system (1.2) reside in $\mathbb{R}^6_+$. □

To prove that the endemic equilibrium state (2.1) is globally asymptotically stable, the Theorem 3.2 shows that the compartments S and I are globally asymptotically stable towards the equilibrium state, i.e.,

$$\begin{aligned}\lim_{t\to\infty} S(t) &= \hat{S} = \frac{N}{R_0},\\ \lim_{t\to\infty} I(t) &= \hat{I} = \frac{\tau N(R_0 - 1)}{\beta},\end{aligned} \tag{4.11}$$

for any initial conditions $S(0) = S_0 \geq 0$ and $I(0) = I_0 \geq 0$ within $\mathbb{R}^2_+$. To prove that the compartments H, U, R, and D are globally asymptotically stable towards the equilibrium state (2.1), we will use the Theorem 4.1 as follows

For the compartment H

$$\lim_{t\to\infty} H(t) = \lim_{t\to\infty}\left(e^{-\sigma_H t}\int_0^t e^{\sigma_H w}\nu I(w)\,dw + e^{-\sigma_H t}H_0\right) = \lim_{t\to\infty}\frac{\int_0^t e^{\sigma_H w}\nu I(w)\,dw}{e^{\sigma_H t}}.$$

Using L'Hospital Rule we obtain

$$\lim_{t\to\infty} H(t) = \lim_{t\to\infty}\frac{e^{\sigma_H t}\nu I(t)}{\sigma_H e^{\sigma_H t}} = \frac{\nu\hat{I}}{\sigma_H} = \frac{\nu\tau N(R_0 - 1)}{\beta\sigma_H} = \hat{H}, \tag{4.12}$$

which shows the global asymptotic stability of the compartment H.

For the compartment U

$$\lim_{t\to\infty} U(t) = \lim_{t\to\infty}\left(e^{-\sigma_U t}\int_0^t e^{\sigma_U w}\eta I(w)\,dw + e^{-\sigma_U t}U_0\right) = \lim_{t\to\infty}\frac{\int_0^t e^{\sigma_U w}\eta I(w)\,dw}{e^{\sigma_U t}}.$$

Using L'Hospital Rule we obtain

$$\lim_{t\to\infty} U(t) = \lim_{t\to\infty}\frac{e^{\sigma_U t}\eta I(t)}{\sigma_U e^{\sigma_U t}} = \frac{\eta\hat{I}}{\sigma_U} = \frac{\eta\tau N(R_0-1)}{\beta\sigma_U} = \hat{U}, \tag{4.13}$$

which shows the global asymptotic stability of the compartment U.

For the compartment R, using L'Hospital Rule we obtain

$$\begin{aligned}\lim_{t\to\infty} R(t) &= \lim_{t\to\infty}\left(e^{-\tau t}\int_0^t e^{\tau w}\left(\alpha_I\gamma_I I(w) + \alpha_H\gamma_H H(w) + \alpha_U\gamma_U U(w)\right)\,dw + e^{-\tau t}R_0\right)\\ &= \lim_{t\to\infty}\frac{\int_0^t e^{\tau w}\left(\alpha_I\gamma_I I(w) + \alpha_H\gamma_H H(w) + \alpha_U\gamma_U U(w)\right)\,dw}{e^{\tau t}}\\ &= \lim_{t\to\infty}\frac{e^{\tau t}\left(\alpha_I\gamma_I I(t) + \alpha_H\gamma_H H(t) + \alpha_U\gamma_U U(t)\right)}{\tau e^{\tau t}}\\ &= \frac{\left(\alpha_I\gamma_I\hat{I} + \alpha_H\gamma_H\hat{H} + \alpha_U\gamma_U\hat{U}\right)}{\tau}\\ &= \frac{N(R_0-1)(\eta\alpha_U\gamma_U\sigma_H + \nu\alpha_H\gamma_H\sigma_U + \alpha_I\gamma_I\sigma_H\sigma_U)}{\beta\sigma_H\sigma_U} = \hat{R},\end{aligned} \tag{4.14}$$

which shows the global asymptotic stability of the compartment R.

For the compartment D, using L'Hospital Rule we obtain

$$\begin{aligned}\lim_{t\to\infty} D(t) &= \lim_{t\to\infty}\left(e^{-dt}\int_0^t e^{dw}\left(\mu_I I(w) + \mu_H H(w) + \mu_U U(w)\right)\,dw + e^{-dt}D_0\right)\\ &= \lim_{t\to\infty}\frac{\int_0^t e^{dw}\left(\mu_I I(w) + \mu_H H(w) + \mu_U U(w)\right)\,dw}{e^{dt}}\\ &= \lim_{t\to\infty}\frac{e^{dt}\left(\mu_I I(t) + \mu_H H(t) + \mu_U U(t)\right)}{de^{dt}} = \frac{\mu_I\hat{I} + \mu_H\hat{H} + \mu_U\hat{U}}{d}\\ &= \frac{\tau N(R_0-1)(\eta\mu_U\sigma_H + \nu\mu_H\sigma_U + \mu_I\sigma_H\sigma_U)}{\beta d\sigma_H\sigma_U} = \hat{D},\end{aligned} \tag{4.15}$$

which shows the global asymptotic stability of the compartment D.

Hence the endemic equilibrium state (2.1) is globally asymptotically stable. □

5. Model (1.2) applied on COVID-19 data

We tested our model (1.2) with data obtained from [19] and other values and trends obtained from statistical literature. We simulated Figure 3*a*, *c*&*d* from [19] and our model provided significant similarities with those figures. We chose the data as shown in Table 1 below.

We chose the initial condition of the system (1.2) following [19]

$$S_0 = N,\ I_0 = 1,\ H_0 = 0,\ U_0 = 0,\ R_0 = 0,\ D_0 = 0. \tag{5.1}$$

Parameters	Values	Data source
N	143.93·1e+7	[19]
β	0.912 (day^{-1})	[19]
τ	1e-5 (day^{-1})	[29]
ν	0.063 (day^{-1})	Assumed
γ_I	$\gamma_{I_0} e^{\delta \gamma_{I_1} t}$	[19]
γ_{I_0}	0.216 (day^{-1})	[19]
γ_{I_1}	0.055 (day^{-1})	[19]
δ	0.82	Assumed
γ_H	γ_I	Assumed
γ_U	γ_I	Assumed
μ_I	$\mu_{I_0} e^{-\xi \mu_{I_1} t}$	[19]
μ_{I_0}	0.035 (day^{-1})	[19]
μ_{I_1}	0.078 (day^{-1})	[19]
ξ	2	Assumed
μ_H	$150\mu_I$	Assumed
μ_U	$150\mu_I$	Assumed
η	0.0145 (day^{-1})	Assumed
α_I	0.1	Assumed recovery in 10 days
α_H	$\alpha_I/2$	Assumed
α_U	$\alpha_I/4$	Assumed
d	7.542·1e-03 (day^{-1})	[5]

TABLE 1. Table of parameters.

Our model provided the following results as shown in Figures 3 & 4. Figure 3 has a very high resemblance with Figure 3$a, c\&d$ from [19] and we used the same time-span used by the authors in [19] i.e., the first 250 days of the COVID-19 pandemic in China, starting February 11, 2020. Additionally, our model provided, in Figure 4, a prediction of the hospitalized and ICU compartments but unfortunately, we did not have available data about hospitalization and ICU to necessarily support these estimates.

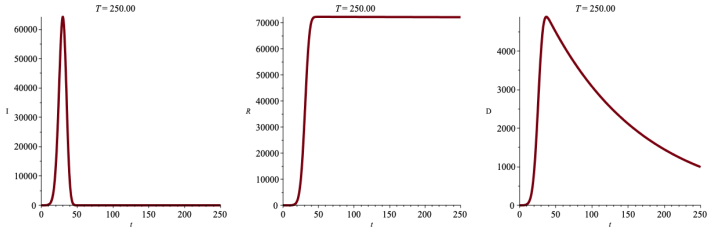

FIGURE 3. The trajectories of the compartments I, R, and D of the system (1.2) with initial conditions (5.1).

As an important exercise for the performance of our model (1.2), we tested it on a pandemic-type scenario with assumed values mentioned in Table 2 below. We

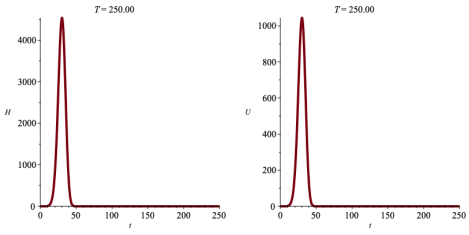

FIGURE 4. The trajectories of the compartments H and U of the system (1.2) with initial conditions (5.1).

considered the data to uniformly represent the global Earth's population (rounded-up from the data declared on June 16, 2021, in [29]) regardless of the geographic location, i.e., we considered all the inhabited geographic areas to be affected in the same way by the pandemic. This scenario is under the assumption that pandemic policies, specifically hospitalization and ICU, would be applied uniformly throughout all inhabited areas. As well, we considered the vital dynamics of the system (1.2) to be the same, globally.

We considered the initial condition of the system (1.2) as follows

$$S_0 = 10^7,\ I_0 = 10^6,\ H_0 = 10^5,\ U_0 = 10^4,\ R_0 = 10^8,\ D_0 = 10^4. \tag{5.2}$$

Figure 5 shows the dynamics of the compartment I with the compartments H, U, R, D from the system (1.2).

Parameters	Values
N	7.57·1e+9
β	0.4417 (month^{-1})
τ	0.000001 (month^{-1})
ν	0.13 (month^{-1})
γ_I	0.1384 (month^{-1})
γ_H	0.3 (month^{-1})
γ_U	0.5 (month^{-1})
μ_I	0.00542 (month^{-1})
μ_H	0.01 (month^{-1})
μ_U	0.08 (month^{-1})
η	0.045 (month^{-1})
$\alpha_{I,H,U}$	1, i.e., assumed recovery in less than 1 month
d	1.05 (month^{-1})

TABLE 2. Table of parameters.

The numerical simulations in Figure 5 revealed that the infection spread "almost" instantaneously, within one month (we considered the time unit to be 1 month). Thus, the model (1.2) fits the "acute epidemicity" factor of COVID-19.

The numerical simulations in Figure 6 show the correlation between hospitalization and ICU and the effect of hospitalization on the recovery and death compartments.

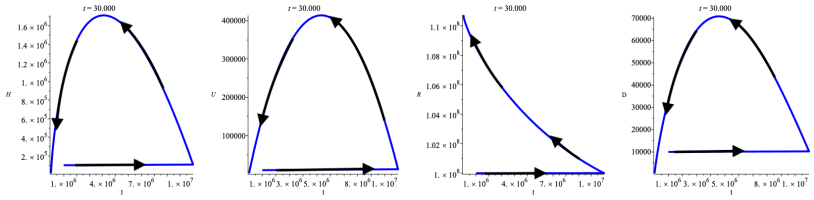

FIGURE 5. The dynamics of the compartment I with the compartments H, U, R, and D, respectively.

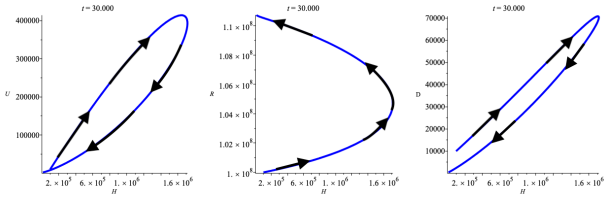

FIGURE 6. The dynamics of the compartment H with the compartments U, R, and D, respectively.

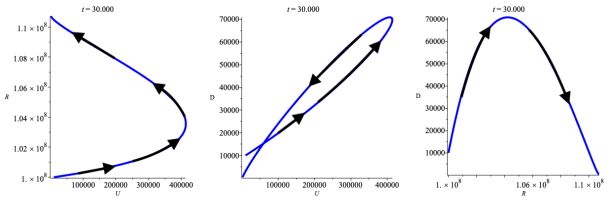

FIGURE 7. The dynamics of the compartment U with the compartments R, and D, respectively, and the dynamics of the compartment R with the compartment D.

Our simulations revealed that the downturn trend (i.e., when H and U start decreasing) is happening after 3 month for the correlation between the hospitalization and ICU. The effect of hospitalization on the recovery compartment shows that while the hospitalization increases, the recovery does increase. After the "wave" passed (which in our simulations turned out to be about 4 month), the hospitalization decreases while the recovery will keep increasing. The effect of hospitalization on the death compartment shows that death will increase during the "wave", after which both hospitalization and death decreased for the remaining time. In our simulations, the "wave" effect of the infection kept consistent at about 4 month.

The numerical simulations in Figure 7 show the effect of ICU on the recovery and death compartments and the correlation between the recovery and death compartments, respectively. For the impact of ICU on the recovery and death compartments, we noticed similar behaviour as the impact of hospitalization on the recovery and

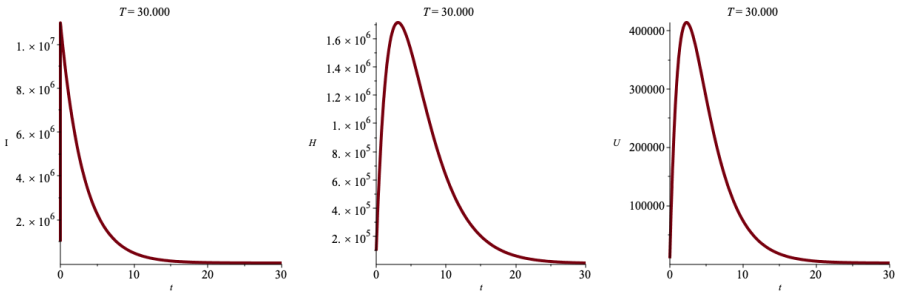

FIGURE 8. The trajectories of the compartments I, H, and U of the system (1.2) with initial conditions (5.2).

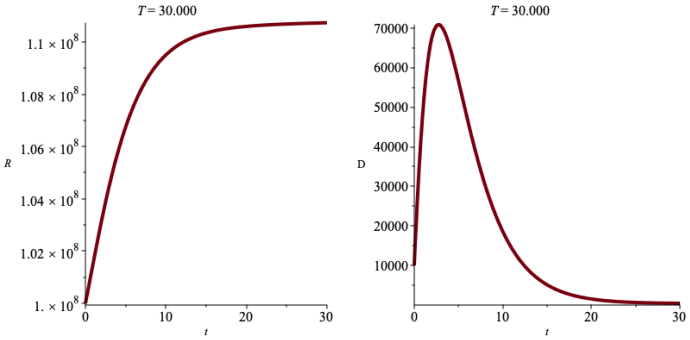

FIGURE 9. The trajectories of the compartments R and D of the system (1.2) with initial conditions (5.2).

death compartments. During the "wave" period, ICU increased while recovery increased and death increased as well, and after the "wave", ICU decreased while recovery kept on increasing and death started decreasing. Let us remember that in the hospitalization compartment, we have individuals who do not require ICU. Our simulations showed that the highest number of deaths occurred during the "wave" period, which was to be expected regarding the correlation between the recovery and death compartments.

Figures 8 & 9 show the trajectories of the compartments I, H, U, R, and D of the system (1.2) with the initial conditions (5.2), which reveal the "wave" period being about 4 month.

6. Summary

In this article, we realized the following main goals

- We proposed a model to describe the dynamics of microparasitic infections, introducing two new compartments for infected human individuals, H and U respectively.
- Our numerical simulations revealed that the proposed model fitted with the expected behaviour of microparasitic infections with "acute epidemicity." The

graphs of the compartments I, H, U, and D are bell-shaped and tend to decline more slowly than they rise [22].

- The numerical simulations presented in Section 5 show consistency in the behaviour of the system (1.2). Thus, we may say that the system has "robust" dynamics. As well, the "robust" dynamics of the model (1.2) is supported by the global stability of its endemic state when $R_0 > 1$. At the same time, the free-disease equilibrium state of (1.2), i.e., when $R_0 \leq 1$ is a globally asymptotic state and the proof is immediate.

The introduction of the compartments H and U in the model (1.2) revealed that it is essential to consider such policies in the case of "acute epidemicity" of microparasitic infections. In our numerical simulations in Section 5, we could not find any data for hospitalization and ICU, except for the microparasitic-induced averaged fatality rate of individuals deceased in ICU, μ_U [18] and we used it in the exercise performed in that section. In both simulations in Section 5, the compartments H and U displayed the expected behaviour of rising fast at the beginning of a "wave" of infections. Once the "wave" has passed, we saw a slower decline for each of them. With our present reality of COVID-19, we noticed that hospitalization and ICU played a critical role (if not crucial) in fighting it. We believe that nations should develop such policies, i. e., hospitalization and ICU, in the circumstances like COVID-19. The measurement of such compartments could improve the understanding of the necessary capacity for hospitalization and ICU in combating microparasitic infections like COVID-19.

This article's primary mission was to bring to the world a new look to a classic SIR model and emphasize the importance of considering the compartments H and I into the "mix" of equations. Thus, in the present paper, we did not focus on parameter estimation. The next step in our research will be to perform parameter estimation and use our model to obtain results based on these estimations.

It is important to mention the preoccupations of statisticians (mainly) in obtaining parameter estimations. For example, in [9] [27] and [7] the authors developed straightforward approaches for parameter estimation based on nonlinear least squares. Other statisticians applied robust methods for analyzing contaminated data to estimate parameters. In [4] the authors applied a robust M-estimator to study parameter estimation for differential equations. As well, in [20] the authors applied a generalized profiling method to estimate parameters for nonlinear ordinary differential equations. In [17] the authors studied large-sample theoretical properties for the methods proposed in [4].

In the exercise performed in Section 5, we used the parameter estimation for β, γ_I, and μ_I from [2], where the authors mentioned that the data on which they performed the parameter estimation was actual data obtained from the Ministry of Health of Brazil between February 25, 2020, to March 30, 2020. Thus, we used the time unit of 1 month. As mentioned, we applied this data uniformly to the whole global population as of June 16, 2021, and the graph for the I-compartment that we obtained in Figure 8 shows some interesting resemblance with the Figure 5 in [2].

For future research, we will estimate the parameters in the model (1.2) by applying the data smoothing methods developed in [20] (see also [4] & [17]). Compared to other popular estimation approaches for ODEs, these methods are advanced in computational efficiency. They are suited to the realization of statistical objectives such as inference and interval estimation, which are also our goals in future research.

We obtained the numerical simulations by using MAPLE software. The initial value problem for the model (1.2) is a stiff problem [8] [24] [25]. We used the Rosenbrock method with relative error 10^{-6}, and the returned procedure was called only for points inside the range on which the method evaluated the numerical solution of the system (1.2) with specified initial conditions. The accuracy of the numerical solutions was also facilitated by increasing the digits environment in MAPLE to 30 (the default digits environment in MAPLE is 10).

References

[1] R.M. Anderson, Discussion: The Kermack-McKendrick epidemic threshold theorem, *Bulletin of Mathematical Biology* **53** (1991), no. 1-2, 3–32.

[2] S.B. Bastos and D.O. Cajueiro, Modeling and forecasting the early evolution of the Covid-19 pandemic in Brazil, *Scientific Reports. Nature Research* **10** (2020), 19457. DOI: 10.1038/s41598-020-76257-1

[3] G.C. Calafiore, C. Novara, and C. Possieri, A time-varying SIRD model for the COVID-19 contagion in Italy, *Annual Reviews in Control* **50** (2020), 361—372. DOI: 10.1016/j.arcontrol.2020.10.005

[4] J. Cao, L. Wang, and J. Xu, Robust estimation for ordinary differential equation models, *Biometrics* **67** (2011), no. 4, 1305–1313. DOI: 10.1111/j.1541-0420.2011.01577.x

[5] China Population 1950-2021. https://www.macrotrends.net/countries/CHN/china/population

[6] C. Castillo-Chavez, Z. Feng, and W. Huang, In: (C. Castillo-Chavez, P. Driessche, D. Kirschner, A.A. Yakubu, editors) *Mathematical Approaches for Emerging and Reemerging Infection Diseases: an Introduction*, Vol. 125, New York: Springer, 2002. 31—65. (The IMA Volumes in Mathematics and Its Applications). eBook ISBN: 978-1-4613-0065-6.

[7] S. Gugushvili and C.A. Klaassen, $\sqrt{n}$-consistent parameter estimation for systems of ordinary differential equations: bypassing numerical integration via smoothing, *Bernoulli* **18** (2012), no. 3, 1061–1098. DOI: 10.3150/11-BEJ362

[8] E. Hairer and G. Wanner, *Solving Ordinary Differential Equations II, Stiff and Differential-Algebraic Problems*, Springer, 1996. ISBN: 3-540-60452-9.

[9] H.C. Hemker, and B. Hess, Analysis and Simulation of Biochemical Systems, Proc. FEBS Meet., North-Holland, Amsterdam, Vol. **25**, 59, 1972.

[10] H.W. Hethcote, Three Basic Epidemiological Models, *Applied Mathematical Ecology*. Springer-Verlag, Berlin, **18** (1989), 119–144. DOI: 10.1007/978-3-642-61317-3_5

[11] H. W. Hethcote, The Mathematics of Infectious Diseases, *SIAM Review* **42** (2000), no. 4, 599–653. DOI: 10.1137/S0036144500371907

[12] K-q. Kam, C.F. Yung, L. Cui, R.T. Pin Lin, T.M. Mak, M. Maiwald, J. Li, C.Y. Chong, K. Nadua, N.W. Hui Tan,, and K.C. Thoon, A Well Infant With Coronavirus Disease 2019 With High Viral Load, *Clinical Infectious Diseases* 71 (2020), no. 15, 847—849. DOI: 10.1093/cid/ciaa201

[13] W.O. Kermack and A.G. McKendrick, A contribution to the mathematical theory of epidemics. *Royal Society. Proceedings of the Royal Society A, Mathematical, Physical and Engineering Sciences* **115** (1927), no. 772, 700–721. DOI: 10.1098/rspa.1927.0118

[14] A. Korobeinikov and P.K. Maini, A Lyapunov Function and Global Properties for SIR and $SEIR$ Epidemiological Models with Nonlinear Incidence, *Mathematical Biosciences and Engineering* **1** (2004), No. 1, 57–60. DOI: 10.3934/mbe.2004.1.57

[15] S. Ma and Y. Xia, *Mathematical Understanding Of Infectious Disease Dynamics*, Lecture Notes Series (National University of Singapore, Institute for Mathematical Sciences) Vol. 16, World Scientific Publishing Company, USA: New Jersey 2009.

[16] V. Martinez, A Modified SIRD Model to Study the Evolution of the COVID-19 Pandemic in Spain, *Symmetry 2021*, 13 (2021), 723. DOI: 10.3390/sym13040723

[17] Y. Qiu, T. Hu, B. Liang, and H. Cui, Robust estimation of parameters in nonlinear ordinary differential equation models, *Journal of Systems Science and Complexity* **29** (2016), no. 1, 41–60. DOI: 10.1007/s11424-015-4045-9

[18] P. Quah, A. Li, and J. Phua, Mortality rates of patients with COVID-19 in the intensive care unit: a systematic review of the emerging literature, *Critical Care* **24** (2020), 285. DOI: 10.1186/s13054-020-03006-1

[19] D. Sen and D. Sen, Use of a Modified SIRD Model to Analyze COVID-19 Data, *Ind. Eng. Chem. Res.* **60** (2021), no. 11, 4251-–4260. DOI: 10.1021/acs.iecr.0c04754

[20] J.O. Ramsay, G. Hooker, D. Campbell, and J. Cao, Parameter estimation for differential equations: a generalized smoothing approach. *Journal of the Royal Statistical Society: Series B (Statistical Methodology)* **69** (2007), no. 5, 741–796. DOI: 10.1111/j.1467-9868.2007.00610.x

[21] R. Ross, An Application of the Theory of Probabilities to the Study of a priory Pathometry - Part I. *Royal Society. Proceedings of the Royal Society A, Mathematical, Physical and Engineering Sciences* **92** (1915), no. 638, 204–730. DOI: 10.1098/rspa.1916.0007

[22] R. Ross and H.P. Hudson, An Application of the Theory of Probabilities to the Study of a priory Pathometry - Part II, *Royal Society. Proceedings of the Royal Society A, Mathematical, Physical and Engineering Sciences* **93** (1917), no. 650, 212–225. DOI: 10.1098/rspa.1917.0014

[23] R. Ross and H.P. Hudson, An Application of the Theory of Probabilities to the Study of a priory Pathometry - Part III, *Royal Society. Proceedings of the Royal Society A, Mathematical, Physical and Engineering Sciences* **89** (1917), no. 621, 225–240. DOI: 10.1098/rspa.1917.0015

[24] L.F. Shampine, Implementation of Rosenbrock Methods, *ACM transactions on Mathematical Software* **8** (1982), no. 2, 93–113. DOI: 10.2172/6754358

[25] L.F. Shampine and R.M. Corless, Initial Value Problems for ODEs in Problem Solving Environments. *Journal of Computational and Applied Mathematics* **125** (2000), 31–40. DOI: 10.1016/S0377-0427(00)00456-8

[26] Z. Shuai and P. van den Driessche, Global stability of infectious disease models using Lyapunov functions, *SIAM Journal on Applied Mathematics* **73** (2013), no. 4, 1513-1532. DOI: 10.1137/120876642

[27] W.J. Stortelder, Parameter estimation in dynamic systems, *Mathematics and Computers in Simulation* **42** (1996), no. 2-3, 135–142. DOI: 10.1016/0378-4754(95)00117-4

[28] P. van den Driessche and J. Watmough, Reproduction numbers and sub-threshold endemic equilibria for compartmental models of disease transmission, *Mathematical Biosciences* **180** (2002), 29–48. DOI: 10.1016/S0025-5564(02)00108-6

[29] World Population Review, https://worldpopulationreview.com

(Ion Bica) Department of Mathematics and Statistics, MacEwan University, 10700-104 Ave NW, Edmonton, AB, T5J 4S2, Canada. ORCHID ID https://orcid.org/0000-0003-0791-3016
E-mail address: bicai@macewan.ca

(Zhichun Zhai) Department of Mathematics and Statistics, MacEwan University, 10700-104 Ave NW, Edmonton, AB, T5J 4S2, Canada. ORCHID ID https://orcid.org/0000-0002-6639-8870
E-mail address: zhaiz2@macewan.ca

(Rui Hu) Department of Mathematics and Statistics, MacEwan University, 10700-104 Ave NW, Edmonton, AB, T5J 4S2, Canada. ORCHID ID https://orcid.org/0000-0003-0371-0166
E-mail address: hur3@macewan.ca